

X-ray Structure of Prephenate Dehydratase from *Streptococcus mutans*

Min Hyung Shin¹, Hyung-Keun Ku²,
Jin Sue Song¹, Saehae Choi¹, Se Young Son¹,
Hee-Dai Kim³, Sook-Kyung Kim²,
Il Yeong Park^{1*}, and Soo Jae Lee^{1*}

¹College of Pharmacy, Chungbuk National University, Chungbuk 361-763, Republic of Korea

²Division of Metrology for Quality of Life, Center for Bioanalysis, Korea Research Institute of Standards and Science, Department of Bio-Analytical Science, University of Science and Technology, Daejeon 305-340, Republic of Korea

³Department of Biotechnology and Bioinformatics, Chungbuk Provincial College, Chungbuk 373-806, Republic of Korea

(Received Dec 16, 2013 / Revised Jan 21, 2014 / Accepted Jan 27, 2014)

Prephenate dehydratase is a key enzyme of the biosynthesis of L-phenylalanine in the organisms that utilize shikimate pathway. Since this enzymatic pathway does not exist in mammals, prephenate dehydratase can provide a new drug targets for antibiotics or herbicide. Prephenate dehydratase is an allosteric enzyme regulated by its end product. The enzyme composed of two domains, catalytic PDT domain located near the N-terminal and regulatory ACT domain located near the C-terminal. The allosteric enzyme is suggested to have two different conformations. When the regulatory molecule, phenylalanine, is not bound to its ACT domain, the catalytic site of PDT domain maintain open (active) state conformation as Sa-PDT structure. And the open state of its catalytic site become closed (allosterically inhibited) state if the regulatory molecule is bound to its ACT domain as Ct-PDT structure. However, the X-ray structure of prephenate dehydratase from *Streptococcus mutans* (Sm-PDT) shows that the catalytic site of Sm-PDT has closed state conformation without phenylalanine molecule bound to its regulatory site. The structure suggests a possibility that the binding of phenylalanine in its regulatory site may not be the only prerequisite for the closed state conformation of Sm-PDT.

Keywords: prephenate dehydratase, X-ray structure, *S. mutans*

Introduction

Microorganisms and plants have autotrophic biosynthetic process that can produce aromatic amino acids such as phenylalanine, tyrosine and tryptophan. Because the aromatic

amino acid biosynthesis is essential for their survival and it is not found in mammals (Husain *et al.*, 2001), the enzymes in the pathway can be good potential targets for antibacterial agents or herbicides. Though there are some other pathways that can produce aromatic amino acid (Xia *et al.*, 1991; Cho *et al.*, 2007), the most well-known and important pathway for the aromatic amino acid biosynthesis is shikimate pathway (Herrmann and Weaver, 1999). In the organisms that utilize shikimate pathway, prephenate dehydratase (EC 4.2.1.51) acts as a key enzyme in the biosynthesis of L-phenylalanine (Bentley, 1990).

Prephenate dehydratase catalyzes the enzymatic conversion of prephenate to phenylpyruvate by decarboxylation and dehydration. Then the phenylpyruvate is converted again to phenylalanine by phenylalanine aminotransferase (Cotton and Gibson, 1965; Bentley, 1990). Prephenate dehydratase was initially found and characterized in bacteria, archaea, fungi, and plants. In Gram-positive bacteria and archaea, prephenate dehydratase exists as monofunctional enzyme, whereas in Gram-negative bacteria, prephenate dehydratase forms a fusion protein with chorismate mutase catalyzing the first two steps of phenylalanine biosynthesis (Bode *et al.*, 1984; Fiske and Kane, 1984; Jensen *et al.*, 1988; Porat *et al.*, 2004; Warpeha *et al.*, 2006).

Prephenate dehydratase is an allosteric enzyme regulated by its end product, L-phenylalanine. The enzyme composed of two domains, catalytic PDT domain located near the N-terminal and regulatory ACT domain located near the C-terminal (Tan *et al.*, 2008). PDT domain can be divided further into PDTa and PDTb subdomain.

Recently, a structural investigation of prephenate dehydratase from *Mycobacterium tuberculosis* (Mt-PDT) by small angle X-ray scattering, ultracentrifugation and molecular modeling reported that prephenate dehydratase is a flat disk protein and exists as tetramer in solution (Tan *et al.*, 2008; Vivan *et al.*, 2008). The elution profile of the size-exclusion chromatography of prephenate dehydratase from *Staphylococcus aureus* (Sa-PDT) and *Chlorobium tepidum* (Ct-PDT) support Vivan's suggestion (Tan *et al.*, 2008; Vivan *et al.*, 2008). And Tan *et al.* (2008) based on the X-ray structures of Sa-PDT and Ct-PDT, proposed the allosteric regulation mechanism of prephenate dehydratase as the conformational changes caused by binding of phenylalanine at the ACT domain propagate to the catalytic site of the enzyme.

In this study, we would like to report a structure of another prephenate dehydratase (PDTa and ACT domain, tentatively designated as Sm-PDT) from *Streptococcus mutans* UA159 (Guo and Shi, 2006), a Gram positive anaerobic bacterium found in human oral cavity involved in tooth decay. Though the Sm-PDT in our crystal does not have the regulatory phenylalanine molecule in its allosteric site, the lower r.m.s. deviation in overall structure and the conformational simi-

*For correspondence. (I.Y. Park) E-mail: parkiy@chungbuk.ac.kr; (S.J. Lee) E-mail: sjlee@chungbuk.ac.kr; Tel.: +82-43-261-2816; Fax: +82-43-268-2732

larity in catalytic site between prephenate dehydratases reveal that the X-ray structure of Sm-PDT is more similar to the closed (allosterically inhibited) state structure of Ct-PDT than the open (active) state structure of Sa-PDT.

Materials and Methods

Preparation of Sm-PDT

Sm-PDT gene was cloned into pET-28a expression vector and transformed in *E. coli* BL21(DE3). The cells were grown at 37°C in seleno-methionine enriched medium M9 and over-expressed at 20°C using 1 mM isopropyl-1-thio- β -D-galactopyranoside (IPTG) for overnight.

Cells were harvested by centrifugation, resuspended in buffer A (20 mM Tris-HCl; pH 7.4, 100 mM NaCl, 10 mM β -mercaptoethanol, 10 mM imidazole) and lysed by sonication with protease inhibitor. After the cell lysate was centrifuged for 20 min, the supernatant was filtered by 0.45 μ m in-line filter (Sartorius, Germany). Filtered protein solution was purified using Ni-NTA affinity column (Qiagen, Germany). Gel filtration chromatography was carried out with a HiLoad™ 26/60 Superdex™ 200 column (GE Healthcare, Sweden), which was pre-equilibrated in buffer B (20 mM Tris-HCl; pH 7.4, 100 mM NaCl, 10 mM β -mercaptoethanol), at a flow rate of 2.0 ml/min. Collected protein solutions were concentrated using Amicon Ultra of 10 kDa cut off, and the concentration of the protein was adjusted to 20.0 mg/ml.

Crystallization and data collection of Sm-PDT

Crystallization was performed by the hanging-drop vapor-diffusion technique at 293K. Hanging drops (2 μ l) were prepared by mixing 1 μ l of the protein complex (containing 20 mM Tris-HCl; pH 7.4) and 1 μ l of reservoir solution. Plate type crystals were obtained from the reservoir condition of

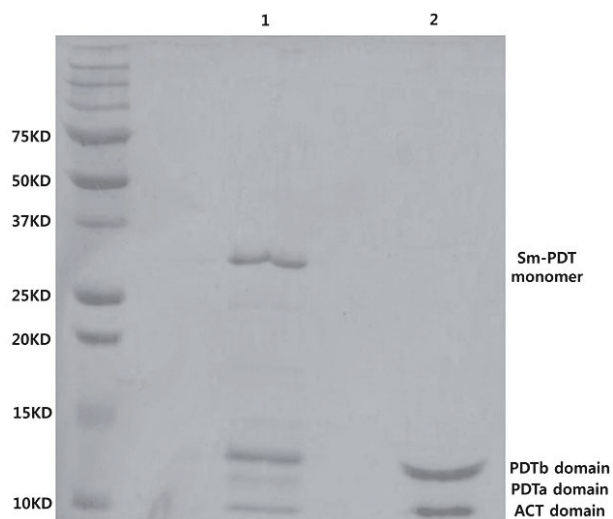


Fig. 1. SDS-PAGE analysis shows that the protein has been cleaved during crystallization process. Lanes: 1, The purified Sm-PDT protein solution after 15 day storage; 2, The re-dissolved Sm-PDT crystal.

15% polyethylene glycol 8000, 100 mM magnesium chloride, 100 mM Tris-HCl pH 7.4 after 15 days. Glycerol solutions of concentration gradient from 5% to 25% (v/v) were used for cryoprotection. Then the crystals were flash-frozen at 100K. X-ray diffraction data were collected at the Pohang Light Source (PLS, beamline 6C1), Korea. The raw data were processed using the HKL2000 software (Otwinowski and Minor, 1997).

Structure determination of Sm-PDT and refinement

The crystal belongs to monoclinic crystal system with C2 space group. The structure was solved by Se-atom single anomalous dispersion (SAD) method and modeled with auto-building option in program Phenix (Adams *et al.*, 2002). COOT and REFMAC5 programs were iteratively used for model building and refinement process (Murshudov *et al.*, 1997; Emsley and Cowtan, 2004). The final atomic coordinates and structure factors have been deposited in the Protein Data Bank, www.pdbj.org (PDB accession code 4LUB). Structural figures were produced using PyMol (www.pymol.org).

Sequence and structure alignment

Sequence alignment of prephenate dehydratases from three organisms was carried out using t-coffee program. The amino acid sequences were obtained from NCBI (www.ncbi.nih.gov). Structural alignment was done by program PSIPRED (McGuffin *et al.*, 2000).

Table 1. Statistics of X-ray diffraction data and structure refinement

	High resolution crystal	Phasing crystal
Data collection		
Space group	C2	C2
Cell dimensions		
a, b, c (Å)	110.81 57.96 85.05	111.69 58.25 83.39
α, β, γ (°)	90.0 125.9 90.0	90.0 124.7 90.0
		<i>Peak</i>
Wavelength	1.2399	0.97972
Resolution (Å)	2.1	2.7
R_{sym} or R_{merge}	0.087 (0.413)	0.141 (0.429)
$I/\sigma I$	14.86 (3.28)	22.6 (3.4)
Completeness (%)	99.6 (97.31)	98.9 (92.5)
Redundancy	3.7 (3.3)	7.0 (6.1)
Refinement		
Resolution (Å)	2.1 (2.18–2.1)	
No. reflections	25695 (2464)	
$R_{\text{work}} / R_{\text{free}}$	0.185 / 0.226	
No. atoms	3199	
Protein	2986	
Water	213	
B -factors	30.20	
Protein	29.8	
Water	36.6	
R.m.s deviations		
Bond length (Å)	0.014	

Results and Discussion

Some fraction of Sm-PDT has been cleft and removed during crystallization

During structure determination, the initial built model contained only ~65% of total 279 amino acids of Sm-PDT, and ~30% of amino acids of the enzyme could not be found till the final stage of refinement. It means that some domain or fragment of Sm-PDT has been removed and is not there in the crystal. Later, it was confirmed by SDS-PAGE (Fig. 1) and MALDI-TOF mass spectroscopy (data not shown).

Sm-PDT seems to be not very stable in β -mercaptoethanol solution. Lane 1 of Fig. 1 shows that, by 15 day storage, some amount of Sm-PDT (31 kDa) in stock buffer solution (20 mM Tris-HCl; pH 7.4, 100 mM NaCl, 10 mM β -mercaptoethanol) has been cleft to 9, 10, and 12 kDa fragment. After obtaining Sm-PDT crystal, the re-dissolved solution of the crystal shows

that there are only 9 and 12 kDa fragments, and not 10 or 31 kDa fragments (Fig. 1, lane 2). The lost 10 kDa fragment is revealed later to be PDTb subdomain, and the antioxidant, β -mercaptoethanol, seems to facilitate the crystallization of Sm-PDT but without the 10 kDa fragment. We tried another antioxidant, dithiothreitol (DTT), however it does not produce any crystal. β -Mercaptoethanol is known to have the ability of breaking disulfide bond of some proteins, but Sm-PDT monomer has only one cysteine and does not have disulfide bond. The mechanism of the cleavage is not clear.

Overall structure of Sm-PDT compared to that of Sa-PDT or Ct-PDT

Sm-PDT consists of three (sub)domains, N-terminal PDTa (residue 5–85, 173–185), PDTb (uncrystallized fragment) subdomain, and C-terminal ACT (residue 186–279) domain. There are two monomers in asymmetric unit related by a

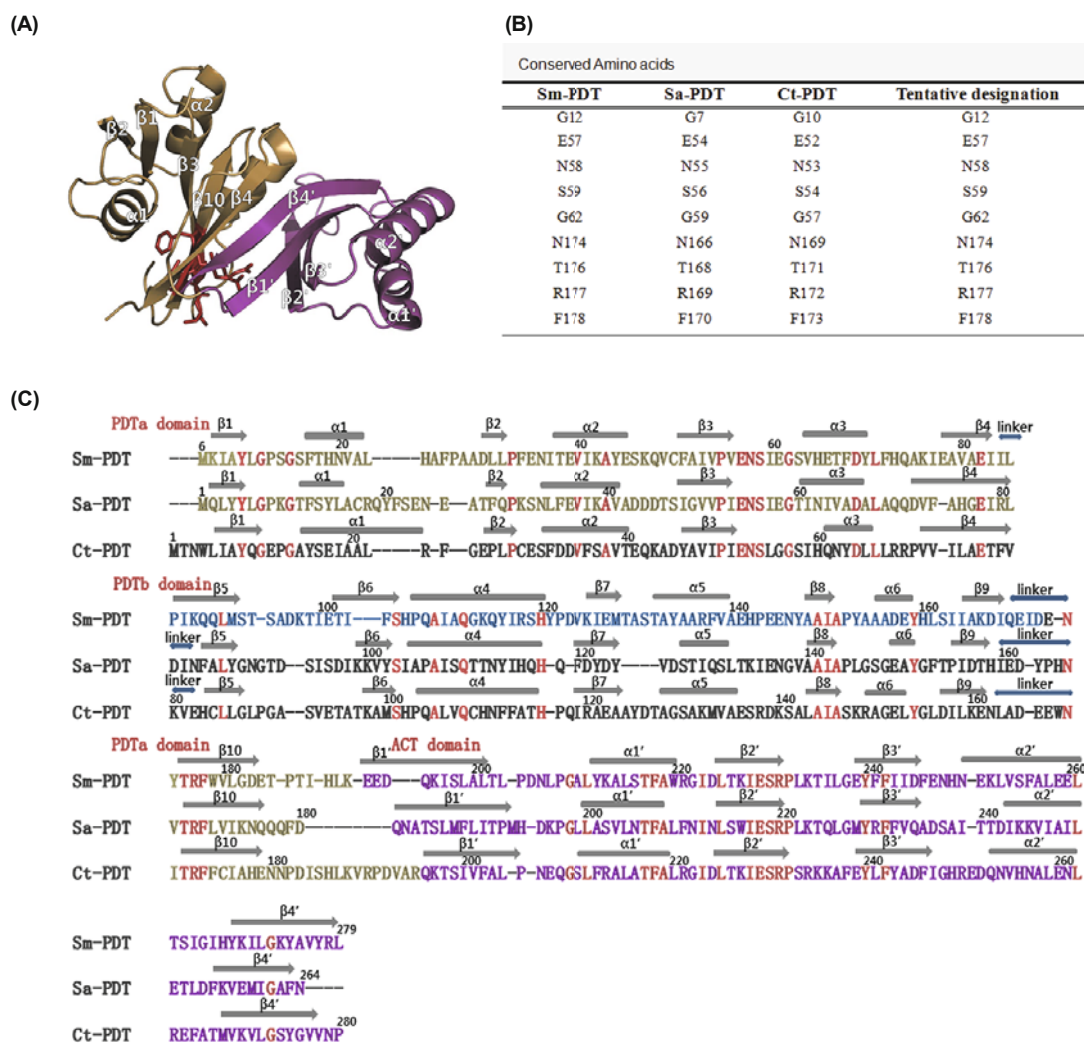


Fig. 2. Sequence alignment and secondary structure of prephenate dehydratase. (A) Cartoon diagram of three-dimensional structure of Sm-PDT monomer. PDTa and ACT domains are shown in mustard and purple, respectively. (B) Some important and conserved amino acid residues and their tentative designation. (C) Multiple sequence alignment of prephenate dehydratases. PDTa and ACT domains are represented in the same color with (A). PDTb domain which was not crystallized in Sm-PDT is shown in blue.

pseudo 2-fold symmetry. PDTa together with PDTb construct the prephenate binding catalytic domain, and ACT is the allosteric regulatory domain to which L-phenylalanine binds (Tan *et al.*, 2008).

The final model of Sm-PDT refined to 19.0/21.8 (R/Free_R factor) and contained protein residues 5-85, 173-279 (PDTa and ACT domain). PDTb subdomain (86-172) could not be determined since it has been cleft and removed during crystallization procedure. In a Ramachandran plot, 96.0% of residues lie in the favored regions, 3.2% in the allowed regions, and 0.8% in the disallowed regions. Data collection and refinement statistics are summarized in Table 1.

The cartoon diagram of the three-dimensional structure of Sm-PDT monomer is shown in Fig. 2A. PDTa subdomain consist of three α helices and five β sheets ($\alpha 1\sim\alpha 3$, $\beta 1\sim\beta 4$, $\beta 10$) and ACT domain consist of two α helices and four β sheets ($\alpha 1'$, $\alpha 2'$, $\beta 1'\sim\beta 4'$). The sequence alignment between Sm-PDT, Sa-PDT, and Ct-PDT is shown in Fig. 2C. The sequence identity of Sm-PDT with Sa-PDT is 32%, and that of Sm-PDT with Ct-PDT is 35%. For clarity purpose, some important and conserved amino acid residue numbers of Sa-PDT and Ct-PDT are tentatively designated as the corresponding equivalent residue numbers of Sm-PDT in this report (Fig. 2B).

Tan *et al.* suggested that the crystal structure of Sa-PDT is the open (active) state of the enzyme, and that of Ct-PDT is the closed (allosterically inhibited) state, on the basis that Ct-PDT has the regulatory phenylalanine molecule bound to its allosteric ACT domain whereas Sa-PDT does not. From the difference between the structures of Ct-PDT and Sa-PDT, they proposed that the conformational changes induced by the binding of phenylalanine are propagated to the catalytic site, and the entrance opening of the catalytic cavity is closed as the result of the conformational changes (Tan *et al.*, 2008; Vivan *et al.*, 2008).

Though Sm-PDT crystal does not contain PDTb subdomain and the primary sequence identity between prephenate dehydratases are low, the folding pattern and quaternary organization between them are nearly same. The overall structure of Sm-PDT (Fig. 3A) show very similar shape to previously reported prephenate dehydratases. For comparison, the three-dimensional structure of Sm-PDT dimer was superimposed to previously reported Sa-PDT and Ct-PDT (Fig. 3B and 3C). Interestingly, the structure of Sm-PDT is more similar to that of Ct-PDT (r.m.s. deviation of 1.5608 Å using corresponding C_{α} atoms) than that of Sa-PDT (r.m.s. deviation of 1.7058 Å).

Regulatory site of ACT domain

The enzymatic activity of prephenate dehydratase is allosterically regulated by its end product, L-phenylalanine. Binding of phenylalanine to the ACT regulatory domain induces conformational change which interrupts prephenate binding into the active site (Pohnert *et al.*, 1999; Prakash *et al.*, 2005). Based on the crystal structures of Sa-PDT and Ct-PDT, Tan *et al.* (2008) proposed that binding of phenylalanine contracts the ACT interface of prephenate dehydratase dimer, and the resulting conformational changes are propagated to the catalytic PDT domain through ACT/PDT interface. The two PDTb subdomain push toward each other and the

two PDTa subdomain move away from each other. As a result, the opening of catalytic cavity shrinks to a small closed state, and the enzyme becomes unable to allow the entrance of the substrate, prephenate.

Fig. 4 shows the phenylalanine binding sites (in regulatory ACT domain) of prephenate dehydratases. A phenylalanine molecule is bound to the allosteric site of Ct-PDT (Fig. 4D). But Sm-PDT (Fig. 4A) and Sa-PDT (Fig. 4C) do not have the regulatory molecule in their allosteric sites. So the structure of regulatory ACT domain of Sm-PDT is more similar to that of Sa-PDT (open, active state) than that of Ct-PDT (closed, allosterically inhibited state).

Catalytic site of PDTa subdomain

A mutagenesis study showed that highly conserved N58 and T176 are crucial residues for catalytic activity (Zhang *et al.*, 2000). Another site-directed mutagenesis study suggested that the highly conserved triplet, T176, R177, F178, is important, and among these, T176 is supposed to be a key residue for the catalytic activity (Hsu *et al.*, 2004).

By the crystal structures of prephenate dehydratases, Tan *et al.* (2008) suggested that the catalytic site of prephenate dehydratase is located at the cleft between PDTa and PDTb subdomain. They showed that the highly conserved triplet, T176, R177, F178, located in $\beta 10$, resides in the catalytic cleft. Around the catalytic site, there are another highly conserved E57, N58, S59 residues (tentatively designated as ENS residue) which seem to control the substrate accessibility to

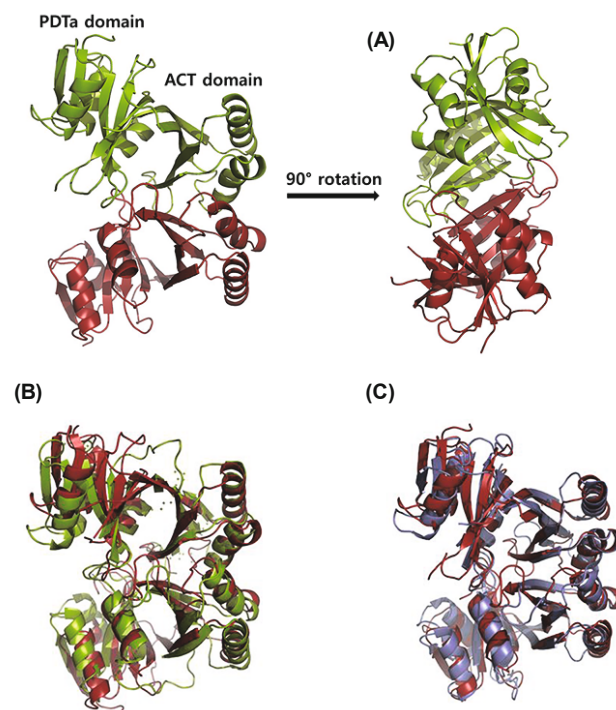


Fig. 3. Comparison of the overall structure of prephenate dehydratase from different bacteria (A) Dimeric structures of Sm-PDT. (B) Overlap diagram of Sm-PDT (red) to Ct-PDT (cyan). (C) Overlap diagram of Sm-PDT (red) and Sa-PDT (green).

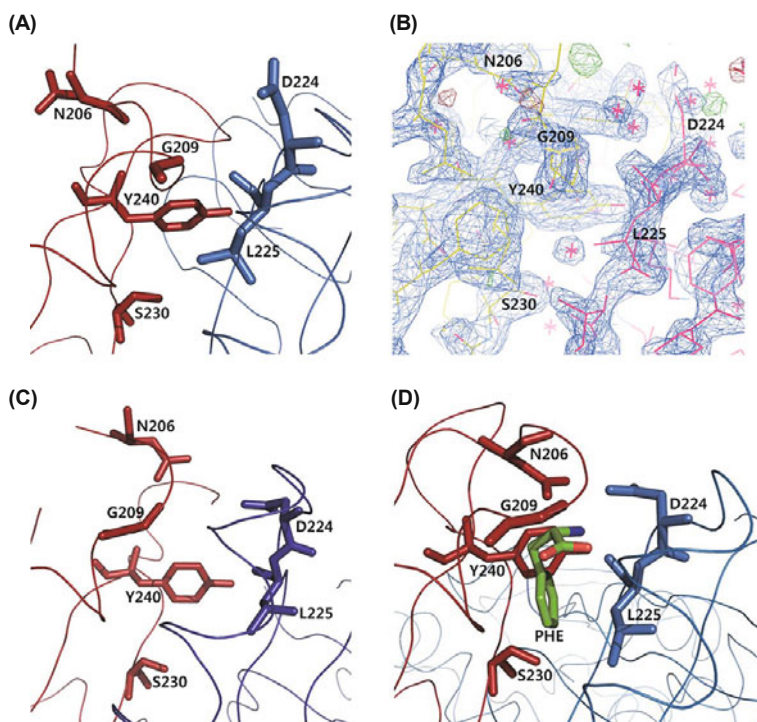


Fig. 4. Detailed structure of regulatory site in ACT domain. Ct-PDT has a phenylalanine molecule at its regulatory site whereas Sm-PDT or Sa-PDT does not. (A) Sm-PDT. (B) The electron-density map around regulatory site of Sm-PDT does not show any foreign molecule except water. (C) Sa-PDT. (D) Ct-PDT.

the catalytic site. The ENS residue is located in $\beta 3$ - $\alpha 3$ loop. Other highly conserved two glycines, G12 and G62, which are located in $\beta 1$ - $\alpha 1$ loop and $\beta 3$ - $\alpha 3$ loop, seem to provide the flexibility for ligand binding (Tan *et al.*, 2008). Although the crystal structure of Sm-PDT does not contain PDTb subdomain, the structure include all the above mentioned residues crucial for catalytic activity (Fig. 2C).

In open state of Sa-PDT, the ENS residue is set aside from substrate binding cavity located between T176 and E61, and do not block the binding of substrate (Fig. 5B) (Tan *et al.*, 2008). A putative prephenate binding model to the catalytic cavity of Sa-PDT crystal structure shows that the substrate may interacts with T176 and E61 of PDTa subdomain (data not shown). However, in closed state of Ct-PDT, the binding of phenylalanine to its regulatory site move the position of the ENS residue, and the ENS residue occupy the catalytic cavity between T176 and E61 (Fig. 5C) inhibiting the substrate entrance into the catalytic cavity. The catalytic key residue of T176 is masked by a hydrogen bond with N58 of ENS residue in Ct-PDT, whereas in Sa-PDT, T176

is not masked and N58 forms a hydrogen bond with highly conserved R220 which locates in ACT domain of another monomer's in asymmetric unit. Interestingly, the structure of Sm-PDT around the catalytic site (Fig. 5A) is quite similar to that of Ct-PDT (Fig. 5C), not to that of Sa-PDT (Fig. 5B). The ENS residue of Sm-PDT occupy the catalytic cavity as that of Ct-PDT, and the catalytic key residue of T176 is masked by a hydrogen bond with E57 of ENS residues, and N58 forms a hydrogen bond with the conserved N174 residue. Although we could not clarify the state of Sm-PDT owing to the absence of PDTb domain in our structure, the structural features show the possibility that Sm-PDT has the closed state conformation in the absence of phenylalanine.

Sm-PDT has closed state conformation without phenylalanine at its allosteric site

Comparisons of Sm-PDT both with Ct-PDT and Sa-PDT show interesting but somewhat confusing features. Sm-PDT does not have the allosteric phenylalanine molecule in its regulatory site, so the structure of regulatory site of Sm-PDT

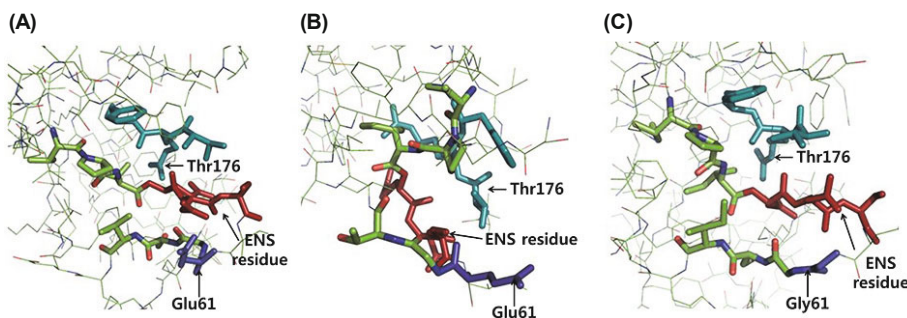


Fig. 5. Detailed structure of catalytic site in PDT domain. The catalytic site of Sa-PDT shows an open conformation, but the opening of the catalytic site of Sm-PDT and Ct-PDT were blocked by ENS residue. (A) Sm-PDT. (B) Sa-PDT. (C) Ct-PDT.

resembles to that of Sa-PDT. However, the structure of catalytic site of Sm-PDT is different from that of active state Sa-PDT, and it is very similar to that of allosterically inhibited state Ct-PDT. The ENS residue covers the catalytic cavity as Ct-PDT, so the substrate is unable to enter the catalytic cavity. The r.m.s. deviation of C α atoms says that the overall structure of Sm-PDT is more similar to that of Ct-PDT than that of Sa-PDT.

Tan *et al.* (2008) suggested the allosteric regulation mechanism as the binding of phenylalanine induces conformational change of prephenate dehydratase, and the propagated conformational change closes the opening of catalytic site. However the crystal structure of Sm-PDT shows that the catalytic site of Sm-PDT has closed state without phenylalanine bound to its regulatory site. Because Sm-PDT is more loose in crystal packing than Sa-PDT or Ct-PDT, there could not be more structural conflict or packing strain that may push each other and change the catalytic site of Sm-PDT. The volume occupied by one monomer of Sm-PDT crystal is about 110,618 Å³, which is far bigger than that of Ct-PDT (78,602 Å³) or Sa-PDT (71,644 Å³). Because the crystallized Sm-PDT does not have PDTb subdomain, it is not clear whether the closed state in catalytic site without phenylalanine bound to its regulatory site is also possible in intact Sm-PDT or not. However the X-ray structure of Sm-PDT suggests a possibility that the binding of L-phenylalanine in its regulatory site may not be the only prerequisite for the closed state conformation of Sm-PDT.

Acknowledgements

This research was supported by the Basic Science Research Program (2010-0003522) through the National Research Foundation of Korea (NRF), the National Research Foundation (NRF) of Korea (2011-0017405) funded by the Korea government (MEST) to S.J.L. and by the research grant of Chungbuk National University in 2010 to I.Y.P..

References

- Adams, P.D., Grosse-Kunstleve, R.W., Hung, L.W., Ioerger, T.R., McCoy, A.J., Moriarty, N.W., Read, R.J., Sacchettini, J.C., Sauter, N.K., and Terwilliger, T.C. 2002. PHENIX: building new software for automated crystallographic structure determination. *Acta Crystallog. D Biol. Crystallogr.* **58**, 1948–1954.
- Bentley, R. 1990. The shikimate pathway--a metabolic tree with many branches. *Crit. Rev. Biochem. Mol. Biol.* **25**, 307–384.
- Bode, R., Melo, C., and Birnbaum, D. 1984. Absolute dependence of phenylalanine and tyrosine biosynthetic enzyme on tryptophan in *Candida maltosa*. *Hoppe Seyler's Z. Physiol. Chem.* **365**, 799–803.
- Cho, M.H., Corea, O.R., Yang, H., Bedgar, D.L., Laskar, D.D., Anterola, A.M., Moog-Anterola, F.A., Hood, R.L., Kohalmi, S.E., Bernards, M.A., and *et al.* 2007. Phenylalanine biosynthesis in *Arabidopsis thaliana*. Identification and characterization of argonate dehydratases. *J. Biol. Chem.* **282**, 30827–30835.
- Cotton, R.G. and Gibson, F. 1965. The biosynthesis of phenylalanine and tyrosine; Enzymes converting chorismic acid into prephenic acid and their relationships to prephenate dehydratase and prephenate dehydrogenase. *Biochim. Biophys. Acta* **100**, 76–88.
- Emsley, P. and Cowtan, K. 2004. Coot: model-building tools for molecular graphics. *Acta Crystallog. D Biol. Crystallogr.* **60**, 2126–2132.
- Fiske, M.J. and Kane, J.F. 1984. Regulation of phenylalanine biosynthesis in *Rhodotorula glutinis*. *J. Bacteriol.* **160**, 676–681.
- Guo, L.H. and Shi, J.N. 2006. Sequencing and bioinformatical analysis of virulent strain-specific DNA fragments from *Streptococcus mutans*. *Hua Xi Kou Qiang Yi Xue Za Zhi* **24**, 541–545.
- Herrmann, K.M. and Weaver, L.M. 1999. The shikimate pathway. *Ann. Rev. Plant Physiol. Plant Mol. Biol.* **50**, 473–503.
- Hsu, S.K., Lin, L.L., Lo, H.H., and Hsu, W.H. 2004. Mutational analysis of feedback inhibition and catalytic sites of prephenate dehydratase from *Corynebacterium glutamicum*. *Arch. Microbiol.* **181**, 237–244.
- Husain, A., Chen, S., Wilson, D.B., and Ganem, B. 2001. A selective inhibitor of *Escherichia coli* prephenate dehydratase. *Bioorg. Med. Chem. Lett.* **11**, 2485–2488.
- Jensen, R.A., d'Amato, T.A., and Hochstein, L.I. 1988. An extreme-halophile archaeobacterium possesses the interlock type of prephenate dehydratase characteristic of the Gram-positive eubacteria. *Arch. Microbiol.* **148**, 365–371.
- McGuffin, L.J., Bryson, K., and Jones, D.T. 2000. The PSIPRED protein structure prediction server. *Bioinformatics* **16**, 404–405.
- Murshudov, G.N., Vagin, A.A., and Dodson, E.J. 1997. Refinement of macromolecular structures by the maximum-likelihood method. *Acta Crystallog. D Biol. Crystallogr.* **53**, 240–255.
- Otwinowski, Z. and Minor, W. 1997. Processing of X-ray diffraction data collected in oscillation mode. vol. 276, pp. 307–326. Elsevier.
- Pohnert, G., Zhang, S., Husain, A., Wilson, D.B., and Ganem, B. 1999. Regulation of phenylalanine biosynthesis. Studies on the mechanism of phenylalanine binding and feedback inhibition in the *Escherichia coli* P-protein. *Biochemistry* **38**, 12212–12217.
- Porat, I., Waters, B.W., Teng, Q., and Whitman, W.B. 2004. Two biosynthetic pathways for aromatic amino acids in the archaeon *Methanococcus maripaludis*. *J. Bacteriol.* **186**, 4940–4950.
- Prakash, P., Pathak, N., and Hasnain, S.E. 2005. pheA (Rv3838c) of *Mycobacterium tuberculosis* encodes an allosterically regulated monofunctional prephenate dehydratase that requires both catalytic and regulatory domains for optimum activity. *J. Biol. Chem.* **280**, 20666–20671.
- Tan, K., Li, H., Zhang, R., Gu, M., Clancy, S.T., and Joachimiak, A. 2008. Structures of open (R) and close (T) states of prephenate dehydratase (PDT)—implication of allosteric regulation by L-phenylalanine. *J. Struct. Biol.* **162**, 94–107.
- Vivan, A.L., Caceres, R.A., Abrego, J.R., Borges, J.C., Ruggiero Neto, J., Ramos, C.H., de Azevedo, W.F., Jr., Basso, L.A., and Santos, D.S. 2008. Structural studies of prephenate dehydratase from *Mycobacterium tuberculosis* H37Rv by SAXS, ultracentrifugation, and computational analysis. *Proteins* **72**, 1352–1362.
- Warpeha, K.M., Lateef, S.S., Lapik, Y., Anderson, M., Lee, B.S., and Kaufman, L.S. 2006. G-protein-coupled receptor 1, G-protein Galpha-subunit 1, and prephenate dehydratase 1 are required for blue light-induced production of phenylalanine in etiolated *Arabidopsis*. *Plant Physiol.* **140**, 844–855.
- Xia, T.H., Ahmad, S., Zhao, G.S., and Jensen, R.A. 1991. A single cyclohexadienyl dehydratase specifies the prephenate dehydratase and argonate dehydratase components of one of two independent pathways to L-phenylalanine in *Erwinia herbicola*. *Arch. Biochem. Biophys.* **286**, 461–465.
- Zhang, S., Wilson, D.B., and Ganem, B. 2000. Probing the catalytic mechanism of prephenate dehydratase by site-directed mutagenesis of the *Escherichia coli* P-protein dehydratase domain. *Biochemistry* **39**, 4722–4728.